

Biogeochemical variability in the upper ocean

A. Mahadevan

Atmospheric and Environmental Research, Lexington, MA - USA

Abstract. Differences in the response times of different biogeochemical tracers to upper ocean forcing processes can lead to substantial differences in their patterns of variability. An idealized tracer with a steep vertical concentration gradient is modeled in a flow field representative of an upper ocean front. The surface distribution of the tracer is studied as a function of its response or restoration time scale.

Introduction

Many quantities, such as temperature, salinity, dissolved inorganic carbon (DIC), nitrate, phosphate, radiocarbon and dissolved oxygen, have strong vertical concentration gradients in the upper 500 or so meters of the ocean. These substances are often forced in the upper ocean, and vertical mixing and transport processes that convey the resulting concentration changes to the ocean interior are extremely small. Horizontal advection, on the other hand, is relatively efficient at mixing and homogenizing substances, and hence concentration gradients are relatively weak in the horizontal. Anomalous concentrations of many biogeochemical quantities in the upper ocean, are therefore, largely a result of upwelling that brings to the surface, water with a substantially different concentration than its surroundings. The substances may also be altered by processes like biological production, remineralization, and air-sea exchange. Such processes could induce horizontal variability, but the variability induced by upwelling is typically smaller scaled, more intermittent, and responsible for most of the variance in the sea-surface distributions of the biogeochemical quantities.

In an earlier modeling study (*Mahadevan and Archer, 2000*), it was observed that the nutrient upwelling rate in the pelagic ocean is very sensitive to model resolution. Increasing the model resolution from 0.4 degrees to 0.1 degrees in a domain situated in the interior of subtropical gyre, resulted in a two- to three-fold increase in not only the mean rate of nutrient supply, but also in the variance of the field. The mean and variance of other model variables like temperature and $p\text{CO}_2$ at the sea surface are not as sensitive to model resolution as new production. The density field in the coarse and fine resolution model runs looks very similar in its mean and variance, but the fine resolution simulation shows more folds in the isopycnal surfaces and greater convolutedness in the frontal outcrop formed by the intersec-

tion of such density surfaces with the euphotic layer. The transport of nutrients from the thermocline into the mixed layer is primarily an isopycnal process. Resolving the length of the front at which the flow field is also highly strained, is thus extremely important for capturing the vertical transport which occurs on scales of the order of 10 km or less.

Even though all the biogeochemical tracers in such a model are affected by vertical motion, the surface distribution of some, for example oxygen and H_2O_2 , appears more fine scaled, i.e., there is more variance at a given length scale than in others like DIC and temperature. While there are many reasons for differences in the distributions of different tracers, I believe that this is largely a result of the difference in the response times of the tracers to various forcing processes. Substances that respond quickly to upper ocean forcing appear in small and intermittent anomalous patches representative of the upwelling scale. When substances are slow to adjust, the anomalous patches introduced by upwelling are stirred and spread by horizontal advection. Hence the distribution of such substances is not as fine-scaled. Carbon dioxide, for example, is very slow to equilibrate with the atmosphere on account of the buffering effect. While the oxygen in a 100m deep mixed layer may typically take one month to equilibrate with the atmosphere, the DIC would take about a year. The surface distribution of oxygen is, as a result, much more patchy or intermittent than DIC.

Modeling Study

The change in distribution of a tracer c in the ocean can be modeled using the equation

$$\frac{\partial c}{\partial t} + \mathbf{u} \cdot \nabla c = S, \quad (1)$$

where \mathbf{u} is the velocity of the fluid and S is a source or sink term. S may parameterize processes like air-sea exchange and biological production that alter the

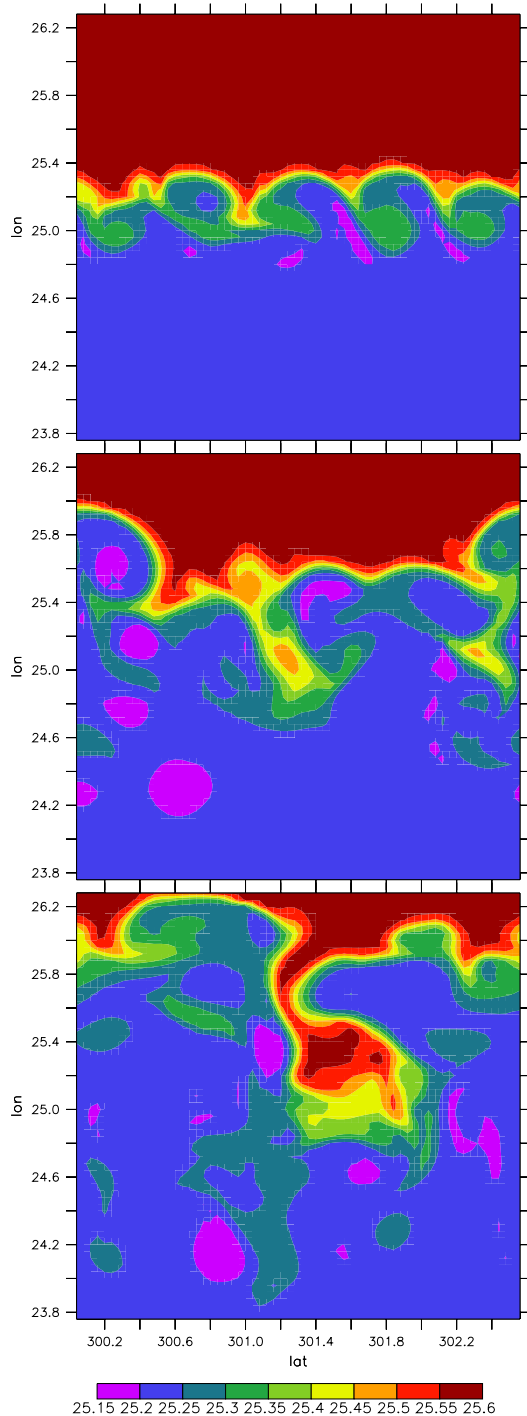


Figure 1. Snapshots of the surface density field in the model shown on days 46, 69 and 93 of the simulation help visualize the evolving flow field. The flow is from west to east along the the density contours.

quantity c . Often S can be expressed in terms of a characteristic response time or adjustment time. In the case of salinity and temperature, S could represent the effect of the heat or evaporation-precipitation flux, and may be expressed as $\lambda^{-1}(c - c_0)$, where c is the temperature or salinity, c_0 is the value to which it is restored at the surface, and λ is the restoration time scale. In the case of nutrients, S may be written as $\lambda^{-1}c_0$, where c_0 may be a combination of the nutrient and light, and λ a biological uptake time. In the case of gases that are subject to air-sea exchange at the ocean surface, S would represent the gas flux, for which the characteristic time scale λ is the ratio of the mixed layer depth to piston velocity. Thus the quantification of the source or sink term S in terms of an adjustment time λ is general to many tracers and processes.

In what follows, we use a three-dimensional numerical model of an idealized ocean front to analyze the surface distribution of a tracer as a function of its response time λ . The tracer c is qualitatively similar to other tracers in the ocean; it has a steep concentration gradient in the upper 500 m. It is modeled using equation (1) which is coupled to the dynamical model described in *Mahadevan et al. (1996)*. The source term on the right hand side of (1) is modeled as

$$S = \begin{cases} 0, & \text{if } z < z_m \\ \lambda^{-1}[c - (1 - \exp(-\frac{z-z_m}{z_0}))], & \text{if } z \geq z_m. \end{cases} \quad (2)$$

Here z is the depth below the surface, z_m can be thought of as a mixed layer or euphotic layer depth, and z_0 is a reference depth. In the absence of advection, the tracer has the steady state profile $c = 1 - \exp(-(z - z_m)/z_0)$ at depths greater than z_m , and a value of 0 at depths less than z_m . The tracer can thus be thought of as depleted in the euphotic layer (z, z_m), and beneath it, increasing exponentially with depth so as to approach 1 over an e-folding distance $z_0 - z_m$. The euphotic depth z_m and e-folding distance $z_0 - z_m$ are each taken to be 100 m in these experiments. Advection disturbs this steady-state distribution to which it is constantly restored with a characteristic adjustment time λ . When λ is small, values of the tracer anomalous from the steady-state exponential distribution are rapidly annihilated. When λ is large, the anomalous values that are introduced primarily by vertical motion, persist for longer, are reinforced by further upwelling, and are spread horizontally by horizontal advection. Diffusion is negligible at the scales considered and is not explicitly included in the model.

The model is set up in a periodic channel with solid north-south boundaries. The domain is approximately 256×284 km in dimension and centered at 25°N . It is initialized with lighter fluid in the upper 100 m of the southern half and denser fluid in the upper northern

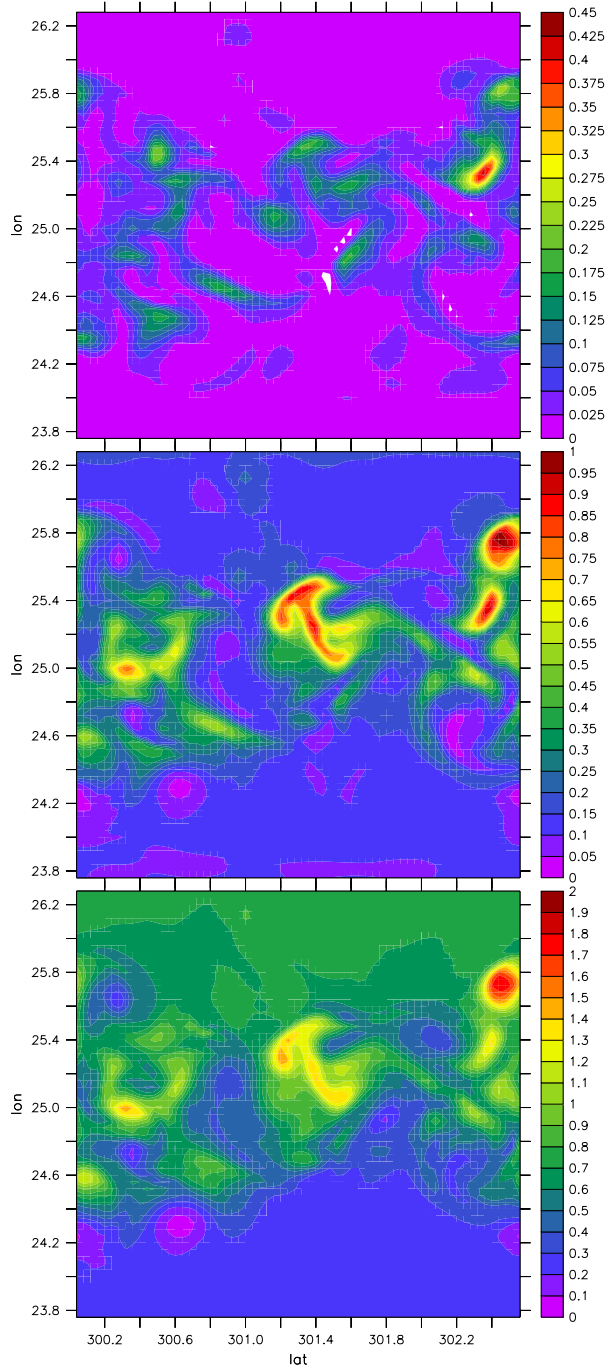


Figure 2. The tracer concentration in the upper 100m viewed on day 69 of the simulation (middle panel of Fig. 1) for three different values of the adjustment time λ : 2.5, 20 and 80 days. The tracer distribution is more patchy and the tracer concentration less for smaller values of λ . The concentration is displayed as a percentage of the maximum concentration, i.e. it is multiplied by 100.

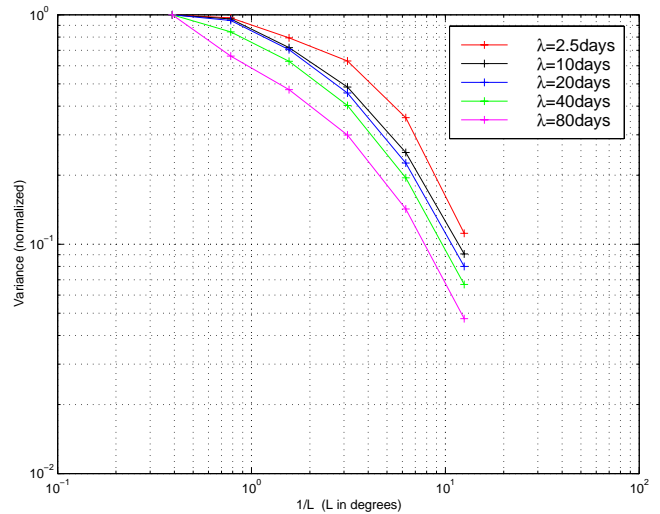


Figure 3. The variance $V(L)$ of the surface distribution of tracer shown in Fig. 2 plotted against wavelength (inverse of the length scale L) on log-log axes for different values of λ . $V(L)$ is the average variance contained in regions of area $L \times L$. Smaller values of λ result in more variance within a given length scale and a shallower curve in the log-log space. The relationship between $V(L)$ and λ seen in this distribution is qualitatively the same at other times in the simulation.

half. Beneath this surface layer, the density in both halves converges to a mean stratification that is representative of the thermocline. The model resolution is 0.04° (approximately 4 km) in the horizontal and varies in the vertical from 10 m near the surface to 125 m at depth. The tracer is initialized to its steady state distribution and allowed to evolve with the flow field. We use five different values of λ : 2.5, 10, 20, 40 and 80 days, and observe differences in the surface distributions of the tracer as a function of λ .

Results

The initial density front gives rise to a geostrophic jet in the along-front direction. The jet and the front meander as the flow evolves giving rise to a more complicated eddy field that gradually decays (Fig. 1). The surface distribution of the tracer that evolves with this flow field varies with λ . It is more patchy and has more variance at a given length scale for smaller values of λ (see Fig. 2). The tracer distributions are analyzed by calculating the variance as a function of length scale [J.W. Campbell, personal communication]. The variance is computed over the whole domain, and then over subregions of size L , by partitioning and re-partitioning the original domain. $V(L)$ is the average variance over all the subdomains of size L that occupy the whole do-

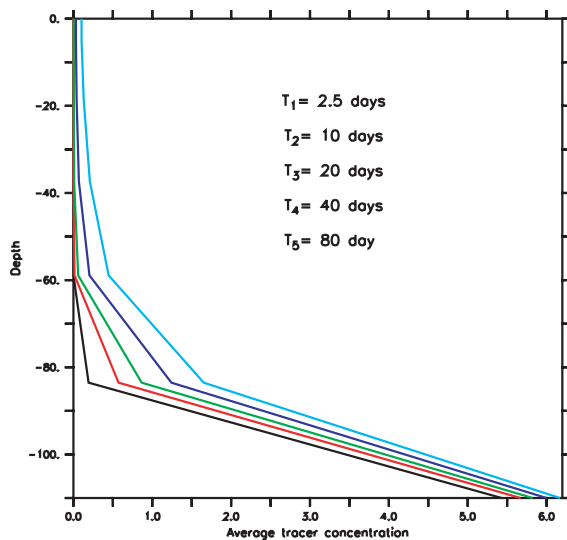


Figure 4. Vertical profiles of the tracer at a late stage (day 93) of the simulation averaged over the domain for different values of λ . The upper ocean tracer concentration increases (at a less than linear rate) with increasing λ .

main. $V(L)$ is normalized by the total variance and plotted as a function of the length scale L on a log-log plot (see Fig. 3). We obtain shallow curves that have small slope when λ is small and steeper curves for large λ . The approximate slope of these curves, denoted by p , is a measure of the intermittency or patchiness of the tracer distribution. Small values of p correspond to a more intermittent or patchy distribution with a large amount of variance at a given length scale. This kind of distribution results from rapid adjustment or small λ . The converse is true for large values of p and λ . The interesting thing is that the increase in p scales roughly as the logarithm of λ .

The same is true for the average anomalous concentration of tracer. Fig. 4 shows the mean vertical distribution of the tracers with different λ towards the end of the simulation. The total amount of tracer in the upper layer ($z < z_m$) increases with λ , but the increase scales roughly as the logarithm of λ for reasons that are not well understood.

balance

Conclusions

Thus it is shown that the distributions of biogeochemical quantities in the upper ocean are sensitive to

their time scale of response to various forcing processes. This ought to be taken into account when trying to design algorithms that quantify the surface distribution of one biogeochemical quantity in terms of another. The patchiness or intermittency of the distribution, quantified here in terms of the approximate slope p of the variance curve in log-log space, increases more or less logarithmically with the adjustment time λ .

Acknowledgments. I am very grateful for the opportunity to be able to participate in this Aha Hulikuo Workshop. My thanks to the conveners of the workshop and to ONR for funding this research.

References

- Mahadevan, A., and D. Archer, Modeling the impact of fronts and mesoscale circulation on the nutrient supply and biogeochemistry of the upper ocean, *J. Geophys. Res.*, *105*, 1209–1225, 2000.
- Mahadevan, A., J. Oliger, and R. Street, A non-hydrostatic mesoscale ocean model 2: Numerical implementation, *J. Phys. Oceanogr.*, *26*, 1181–1900, 1996.
- A. Mahadevan, Atmospheric and Environmental Research, 131 Hartwell Avenue, Lexington, MA 02421 (e-mail: amala@aer.com)

This preprint was prepared with AGU’s L^AT_EX macros v4, with the extension package ‘AGU++’ by P. W. Daly, version 1.6a from 1999/05/21, with modifications by D. E. Kelley, version 1.0 from 2001/03/26, for the ‘Aha Huliko’a Hawaiian Winter Workshop.